water

MDPI

Article

Suspended Sediment Load Simulation during Flood Events Using Intelligent Systems: A Case Study on Semiarid Regions of Mediterranean Basin

Zaki Abda [1,*], Bilel Zerouali [2,*], Muwaffaq Alqurashi [3], Mohamed Chettih [1], Celso Augusto Guimarães Santos [4] and Enas E. Hussein [5]

1 Research Laboratory of Water Resources, Soil and Environment, Department of Civil Engineering, Faculty of Civil Engineering and Architecture, Amar Telidji University, P.O. Box 37.G, Laghouat 03000, Algeria; m.chettih@lagh-univ.dz
2 Vegetable Chemistry-Water-Energy Research Laboratory, Faculty of Civil Engineering and Architecture, Hassiba Benbouali, University of Chlef, B.P. 78C, Ouled Fares, Chlef 02180, Algeria
3 Department of Civil Engineering, College of Engineering, Taif University, Taif 21944, Saudi Arabia; m.gourashi@tu.edu.sa
4 Department of Civil and Environmental Engineering, Federal University of Paraíba, João Pessoa 58051-900, Brazil; celso@ct.ufpb.br
5 Water Research Center, P.O. Box 74, Shubra El-Kheima 13411, Egypt; enas_el-sayed@nwrc.gov.eg
* Correspondence: z.abda@lagh-univ.dz (Z.A.); b.zerouali@univ-chlef.dz (B.Z.)

Abstract: Sediment transport in rivers is a nonlinear natural phenomenon, which can harm the environment and hydraulic structures and is one of the main reasons for the dams' siltation. In this paper, the following artificial intelligence approaches were used to simulate the suspended sediment load (SSL) during periods of flood events in the northeastern Algerian river basins: artificial neural network combined with particle swarm optimization (ANN-PSO), adaptive neuro-fuzzy inference system combined with particle swarm optimization (ANFIS-PSO), random forest (RF), and long short-term memory (LSTM). The comparison of the prediction accuracies of such different intelligent system approaches revealed that ANN-PSO, RF, and LSTM satisfactorily simulated the nonlinear process of SSL. Carefully comparing the results, the ANN-PSO model showed a slight superiority over the RF and LSTM models, with RMSE = 67.2990 kg/s in the Chemourah basin and RMSE = 55.8737 kg/s in the Gareat el tarf basin.

Keywords: SSL; artificial intelligence; LSTM; PSO; ANFIS; random forest

check for updates

Citation: Abda, Z.; Zerouali, B.; Alqurashi, M.; Chettih, M.; Santos, C.A.G.; Hussein, E.E. Suspended Sediment Load Simulation during Flood Events Using Intelligent Systems: A Case Study on Semiarid Regions of Mediterranean Basin. *Water* **2021**, *13*, 3539. https://doi.org/10.3390/w13243539

Academic Editor: Giuseppe Pezzinga

Received: 14 November 2021
Accepted: 8 December 2021
Published: 10 December 2021

Publisher's Note: MDPI stays neutral with regard to jurisdictional claims in published maps and institutional affiliations.

Copyright: © 2021 by the authors. Licensee MDPI, Basel, Switzerland. This article is an open access article distributed under the terms and conditions of the Creative Commons Attribution (CC BY) license (https://creativecommons.org/licenses/by/4.0/).

1. Introduction

Many significant threats to water resources arise primarily from human activities, including pollution, climate change, urbanization, and landscape changes. Each one has specific impacts, and most are often directly on ecosystems with repercussions on water resources [1]. In sedimentology, sediment transport in a river is a nonlinear and complex phenomenon, is more active during flood periods that cause a more significant amount of sediment, and is very varied in space and time. The geological, hydrological, and morphological parameters of a river basin have substantial implications on the sediment activity inside a river [2]. According to Zounemat-Kermani et al. (2016) [3], suspended sediment load (SSL) and bed sediment load (BSL) are the two significant parts of sediment load. Still, the SSL has a complex behavior compared to BSL and can be considered the most crucial part of the sediment load [4]. In hydraulic engineering, before installing hydraulic structures, such as dams and reservoirs, the study and estimation of the volume of sediment transported constitutes an important issue and is of particular interest in the final decision [2,5]. The economic life of a reservoir is expressed through dead storage by the incoming sediments. A poor estimate of the sediment volume results in insufficient dam capacity [5], requiring maintenance and cleaning procedures, such as dredging.

However, those procedures are costly and sometimes even exceed the cost of rebuilding the structure itself. Toumi and Remini (2018) [6] highlight an accumulated silt deposit of more than 650,106 m^3 in more than 110 Algerian dams. For example, a silt volume equal to 100 million m^3 is currently at the bottom of the Sidi M'hamed Ben Aouda dam (Algeria), representing a filling rate equal to 42%. This value places it among the dams most threatened by siltation [7].

Traditionally, the relationship between discharge and sediment concentration, for example, has been based on setting up a simple linear regression model. This linear relationship based on empirical equations does not represent reality due to the spatiotemporal variability of the data; the notable disadvantage of these equations leads to estimates with a considerable margin of error [8]. Although, since the end of the 1980s, this linear relationship seems to be an up-and-coming technique to model the runoff–sediment load relationship to improve water resources infrastructure planning, a new concept of nonlinear empirical and conceptual models based on artificial intelligence seems to constitute an innovative approach to model complex systems [9]. The success of artificial intelligence techniques to model complex systems, since the first use of classical models of artificial neural networks (ANN), has led researchers to develop robust systems. Some examples are the intelligent hybrid systems that combine optimization and probabilistic reasoning techniques, known universally as soft computing [10]. The significant advantage of these systems is reasoning and learning in an imprecise and uncertain environment [11]. In the context of SSL, the following works can be mentioned: [12–25]. Meshram et al. (2019) [25] used the two-phase feed-forward neuron network particle swarm optimization gravitational search algorithm (FNN-PSOGSA), the single-phase feed-forward neuron network particle swarm optimization (FNN-PSO), feed-forward neuron network (FNN), and adaptive neuro-fuzzy inference system (ANFIS) to estimate monthly sediment load. The authors found that the FNN-PSOGSA model was superior to the other models. Kumar et al. (2016) [26] used the machine learning approach for daily SSL simulation in the Kopili River basin (India). The assessment indicates that the least square support vector regression (LS-SVR) and ANN offer more insight than decision tree models such as the M5 model tree and classification and regression tree (CART). Based on ANN, ANFIS, and support vector machine (SVM) models, SSL in the Coruh River (Turkey) was estimated by Buyukyildiz and Kumcu (2017) [19]. Yilmaz et al. (2019) [23] used hybrid artificial intelligence techniques combining ANN with teaching–learning-based optimization (TLBO) and artificial bee colony (ABC) for SSL prediction. The results of ANN-TLBO and ANN-ABC models are more promising than the classical ANN model for SSL prediction. For suspended sediment concentration (SSC) prediction, Kisi and Yaseen (2019) [21] have documented the effectiveness of the hybrid evolutionary fuzzy (EF) intelligence model. The conjunction between subtractive clustering (SC), grid partition (GP), and fuzzy c-means (FCM) models with an adaptive neuro-fuzzy inference system (ANFIS) indicates the high qualification of the proposed models to be a brilliant approach for SSC prediction. Nourani et al. (2019) [22] used a wavelet-based data mining technique for SSL simulation. The different modeling approaches found that the Wavelet-M5 tree model predicts SSL with high reliability compared with Wavelet-ANN (WANN) and M5 tree models. Adnan et al. (2019) [27] used dynamic evolving ANFIS (DENFIS), ANFIS-FCM, and multivariate adaptive regression splines (MARS) for SSL prediction, in Guangyuan and Beibei (China). The comparison between different approaches demonstrates that the DENFIS can be the best approach for the accurate estimation of SSL. Banadkooki et al. (2020) [28] used ANN models based on ant lion optimization (ALO), bat algorithm (BA) and particle swarm optimization (PSO)for SSL prediction. The results indicates that the ANN-ALO improved the accuracy RMSE of the ANN-BA and ANN-PSO models by 18% and 26%, respectively. In three rivers in Idaho (United States), an assessment of sediment load forecasting using ANN was performed with different sensitivity analysis methods and 263 processed datasets. Applying the nine sediment variables and different measured flows with sensitivity analysis indicated no good relationship between suspended load and predicted bedload [24]. Salih et al.

(2020) [4] used newly developed data mining models for river SSL prediction based on M5P, M5Rule (M5R), attribute selected classifier (AS M5P), and K Star (KS). Overall, the results obtained achieved excellent forecasting of the SSL process. The results obtained show good reliability for different use approaches. Kaveh et al. (2020) [29] used long short-term memory (LSTM) for daily SSC prediction in Schuylkill River (United States). The comparison was made between the ANN, ANFIS, and LSTM models. The results show that the LSTM could be very satisfactory for SSC time series prediction.

In Algeria, the population faces a water shortage situation [30], with a capital of less than 500 m^3/inhabitant/year [31]. Therefore, it is well below the threshold that separates countries in the red from those with relative sufficiency [31]. Despite the various development programs carried out in the early 2000s, a considerable breakthrough has been achieved in constructing mobilization works, including more than 94 dams in operation, and 5 in progress, for a total capacity of 8.4 billion m^3. The situation in terms of the protection and control of storage volumes and dead volumes of these structures, for example, is not under control. This situation requires a national emergency response program to optimize water resource mobilization structures [32]. Suspended sediments transported across rivers are a significant cause of this situation and other environmental impacts, which is well explained by Buyukyildiz and Kumcu (2017) [19]. The studies carried out in the context of SSL at the basin level in Algeria are not sufficient by comparing with its area and the number of dams in operation (e.g., [7,33–38]).

For example, in the Sacramento River (California), Nakato (1990) [36] tested a set of sediment-transport formulas, i.e., the Ackers–White Einstein–Brown, Engelund–Fredsoe, Engelund–Hansen, Inglis–Lacey, Karim, Meyer–Peter and Mueller, Rijin, Schoklitsch, Toffaleti, and Yang formulas. The study results clearly show how difficult it is to predict the sediment discharge in natural rivers. In the Yellow River, China, Baosheng et al. (2008) [33] evaluated the applicability of the sediment transport methods developed by Engelund and Hansen, Ackers and White, Yang et al., and van Rijn, and compared with the Wuhan methods. The results show that the best possible predictions were obtained by the Yang et al., Wuhan, and modified Wuhan methods. Acceptably good predictions were also obtained by the van Rijn method. Several studies predict SSL based on artificial intelligence systems, as ANN models are the most widely used intelligent models in this field [39–42]. This paper assessed four approaches, ANN-PSO, ANFIS-PSO, RF, and LSTM, for estimating SSL at Chemourah and Gueiss wadis. This analysis was performed in an information-scarce environment, which is what the researcher and practitioner suffer in Algeria. Therefore, the main aim of this study was to make essential decisions with scant information.

2. Materials and Methods

2.1. Artificial Neural Networks

ANN can be defined as a reasoning model inspired by biological neural networks based on the human brain. It is a relatively nonlinear technique that belongs to the black box model category. ANN is a set of interconnected artificial neurons that perform nonlinear mathematical functions for information processing. Many distinct neural networks are characterized by their activation function and how interconnection is achieved between neurons. Among these types is the multilayer perceptron (MLP). The MLP is a neural network among the most popular models of ANN [43], and is a feedforward network with multiple layers. It consists of an input layer, one or more hidden layers, and an output layer. Each layer contains neurons' propagated signals (connections) in a forward direction layer by layer since there is no connection to neurons from the same layer. In Figure 1 is shown the structure of the multilayer perceptron. The learning of MLP is supervised by minimizing the cost function, which is the sum of squared errors that represent the differences between the observed and simulated values of the network. Backpropagation was the selected algorithm for training MLP to measure the difference between the observed and simulated values of the network and propagate. The problem

of the slowness of classical backpropagation led to the emergence of several different algorithms. Among these is the Levendberg Marquardt backpropagation (LMBP). In the context of our work, we use the LMBP algorithm because of its efficiency [44,45].

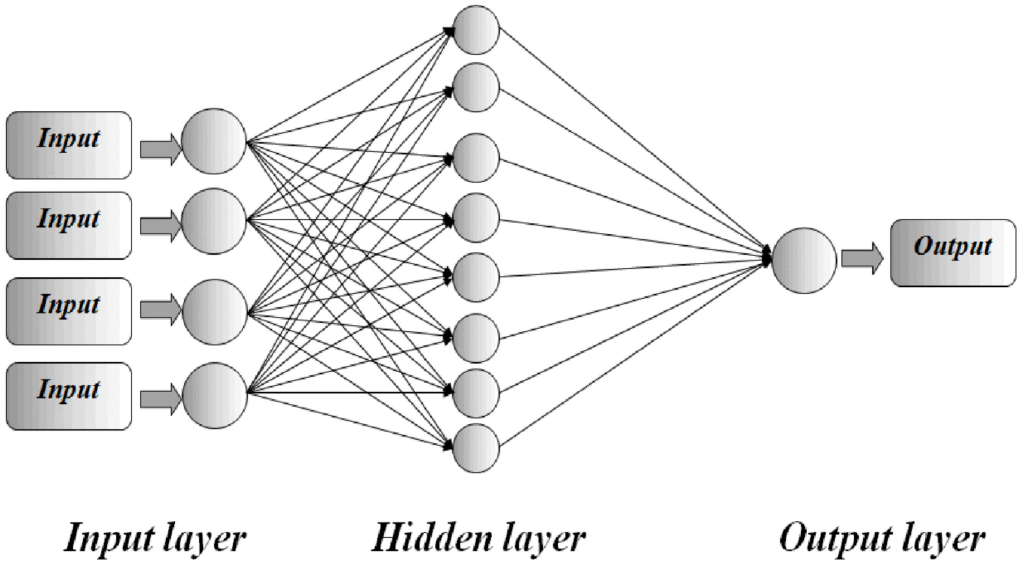

Figure 1. Structure of multilayer perceptron neural networks.

2.2. Neuro-Fuzzy Inference Systems

The adaptive neuro-fuzzy inference system (ANFIS) is an intelligent hybrid model combining ANN and fuzzy inference systems. It is a black box nonlinear mathematical technique capable of forming relationships between the inputs and outputs of a system, which was first introduced by Jang (1993) [46]. ANFIS is an MLP neural network equivalent to a fuzzy system structure, i.e., ANFIS applies the learning mechanism of ANN (back-propagation learning) on fuzzy inference techniques. ANFIS is a neuro-fuzzy inference model of the Sugeno type [47,48]. It can define parameters of membership functions and fuzzy rules (if, then) from the inputs and outputs of the system, as described in Figure 2a.

$$\text{Rule 1}: \text{ If } x \text{ is } A_1 \text{ and } y \text{ is } B_1, \text{ then } Z_1 = a_1 x + b_1 y + c_1 \quad (1)$$

$$\text{Rule 2}: \text{ If } x \text{ is } A_2 \text{ and } y \text{ is } B_2, \text{ then } Z_2 = a_2 x + b_2 y + c_2 \quad (2)$$

where A_i and B_i are fuzzy sets and a_i, b_i, and c_i are the consequent parameters determined during the learning process [49,50].

As shown in Figure 2b, the architecture of the ANFIS model has five layers: the fuzzification layer, the rules layer, the normalization layer, the defuzzification layer, and the summation layer.

2.3. Particle Swarm Optimization

Particle swarm optimization (PSO) is a metaheuristic optimization algorithm that is somewhat similar to evolutionary computations. It was first invented by Kennedy and Eberhart (1995) [51]. PSO is an optimization algorithm that relies on a population of candidate solutions (called particles) to develop the optimal solution of the problem. It was initially inspired by the living world, specifically by simulating the social behavior of animals, such as flocks of birds, fish, or bees. This algorithm aims to graphically simulate the graceful and unpredictable choreography of bird individuals. Each individual in the swarm is represented by a vector in the multidimensional search space. This vector also has a custom vector that defines the subsequent movement of the particle, called the velocity vector. In addition, each particle contains a memory that allows it to

remember its best performance in value and location and the best performance achieved by neighboring particles.

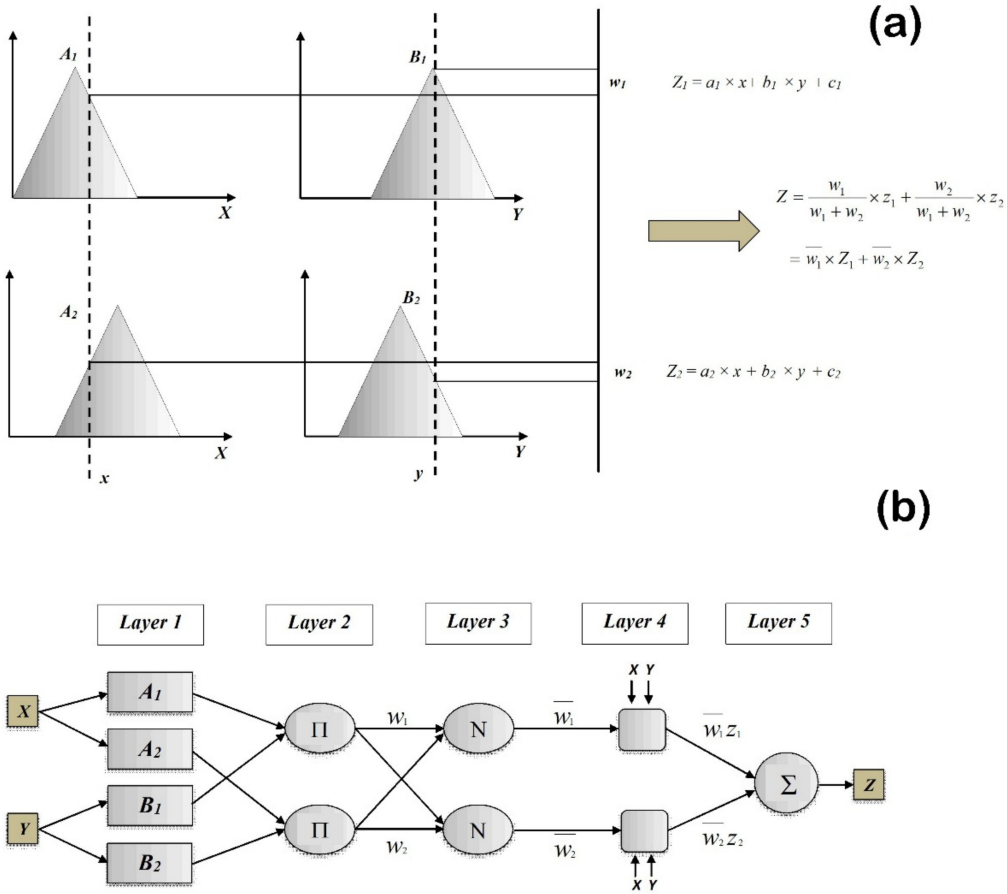

Figure 2. (**a**) Sugeno fuzzy reasoning and (**b**) architecture of ANFIS.

At the start of the algorithm, each particle is placed in the search space. The movement of particles for each iteration is affected by three components:

1. The current velocity.
2. The best performance.
3. The best performance in its neighborhoods.

The general principle of PSO functioning is illustrated in Figure 3.

2.4. Random Forest

Random forests (RF) or forest of decision trees are techniques that provide predictive models for classification and regression. To do this, they combine many decision trees in a bagging-type approach. This technique was introduced by Leo Breiman [52], who suggested it earlier under the name of CART trees (1984). RF implements binary decision trees (CART). It performs parallel learning on multiple decision trees built randomly and trained on different data subsets. In statistical terms, if the trees are decorrelated, it helps reduce the forecasts' variance. The working principle of the RF technique is illustrated in Figure 4.

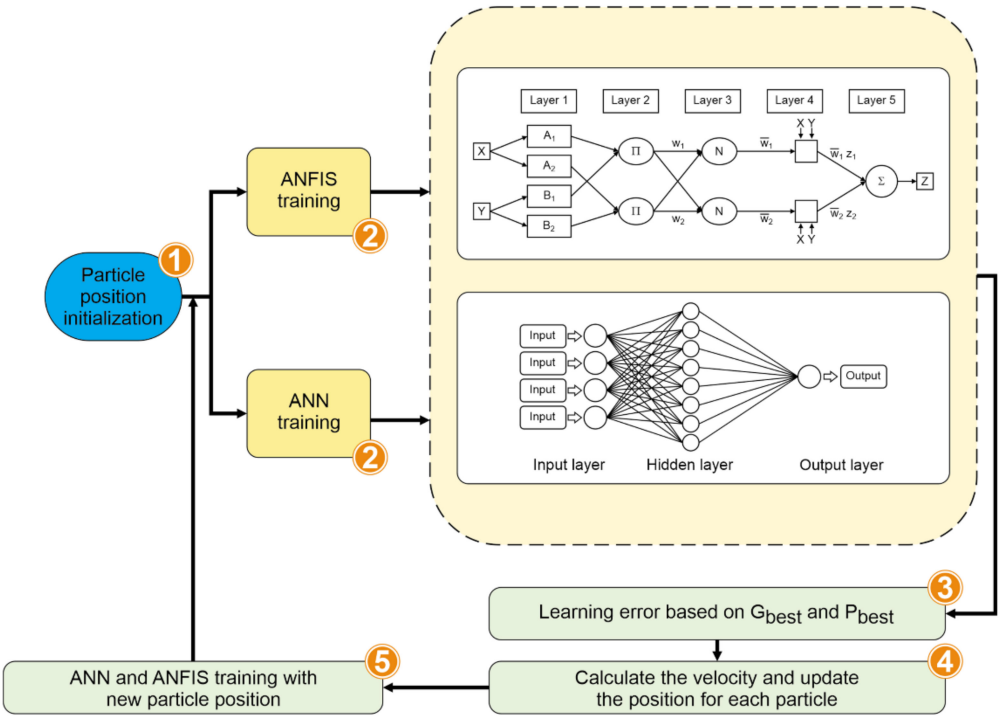

Figure 3. Structure of the ANN-PSO and ANFIS-PSO models.

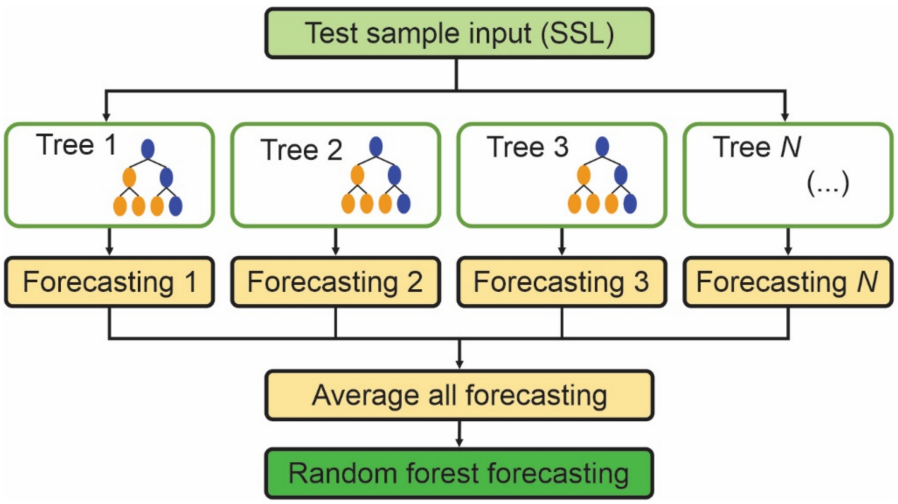

Figure 4. Flowchart of the RF functioning.

The following equation represents the output of the regression model, which is the average of all the predicted values of the decision trees:

$$h(X) = \frac{1}{K}\sum_{k=1}^{K} h(x, \theta_k) \tag{3}$$

where K is the number of regression trees (k = 1, 2, . . . , K), x is a subset of the training dataset X (input series), θ are normally distributed random variables (with zero mean and unity variance) of the combined classifier, and $h(x, \theta_k)$ is the generated decision tree based on x and θ_k.

2.5. Long Short-Term Memory Networks

Long short-term memory networks (LSTM) (Figure 5) are an extension for recurrent neural networks (RNN), which expands their memory. Therefore, they are well suited for learning from essential experiences, which have very long delays in between. The units of an LSTM that have internal memory are used as building units for the layers of an RNN, which is then often referred to as an LSTM network. This unit consists of a numeric value that the network can drive based on situations.

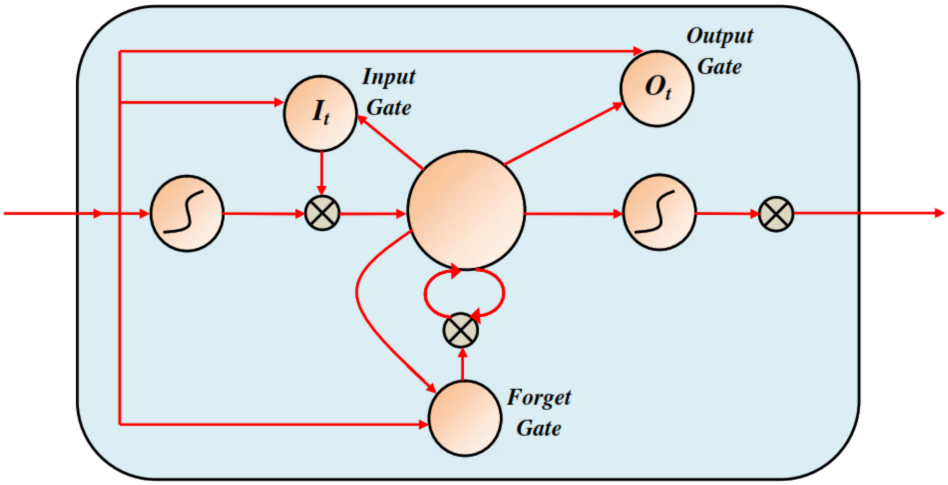

Figure 5. Flowchart of the LSTM functioning.

An LSTM neuron comprises an internal memory controlled by three gates: an input gate, an output gate, and a forget gate. The input gate decides whether or not to let a new entrance input, and the forget gate decides whether to delete the information and reset the unit contents to 0. The output gate determines whether the unit contents must influence the neuron's output at the current time. Figure 4 shows a schematic of an LSTM neuron. The type of algorithm for learning LSTM is backpropagation through time (BPTT), as in classic recurrent networks, by unfolding the recurrent network over time.

2.6. Data Sources

For a good SSL estimation, several parameters must be used. In this study, a great lack of necessary information and data was faced. However, it was possible to use the liquid flow and solid flow data recorded during flood periods.

The flows and SSL data were obtained from Foum El Gueiss and Chemourah gauging stations in the Gareat el tarf and Chemorah basins, respectively, provided by the National Agency of Hydraulic Resources. Foum El Gueiss gauging station provides 26 years of data, and the Chemourah station provides only 13 years of data recorded during flood periods.

3. Study Area

The Gareat el tarf and Chemorah basins are located in the northeastern part of Algeria, at the extreme east of the high steppe plains between the Tellian Atlas in the north and the Saharan Atlas in the south. It is a part of the basins of Constantine's highlands, according to the National Agency of Hydraulic Resources (ANRH). The Gareat el tarf basin is located between the northern latitudes 35°22′ and 35°56′ and the eastern longitudes 06°49′ and 07°34′, where Oued Chemora is situated at 35°39′52″ N and 6°38′41″ E. The Gareat el tarf basin covers an area of 2432 km^2 [53], whereas the Chemorah basin has an area of 755 km^2.

The Gareat el tarf and Chemorah basins (Figure 6) are limited to the north by the Sidi Reghis and Aamamet El Kebir massifs, to the south by the Feraoun, Aurès, and El Aoud mountains, to the east by the Fedjidjet, Bou Tokhma, Tafrennt, and Chettaia massifs, and to the west by the Fedjoudj and Tarf mountains. The Gareat el tarf basin constitutes a

pervasive and relatively high endorheic depression, about 960 m, receiving all the erosion inputs from the surrounding reliefs. Most of the rivers in the basin flow towards the lake of Gareat el tarf. In general, two types of climate characterize the Gareat el tarf basin: The north is covered by a semiarid climate, and the south is affected by cold and humid air currents from the Aurès, resulting in a temperate climate [53]. The Chemorah basin has almost the same characteristics as the Gareat el tarf basin, as they are affected by a semiarid Mediterranean climate with a cold and wet winter and dry and hot summer.

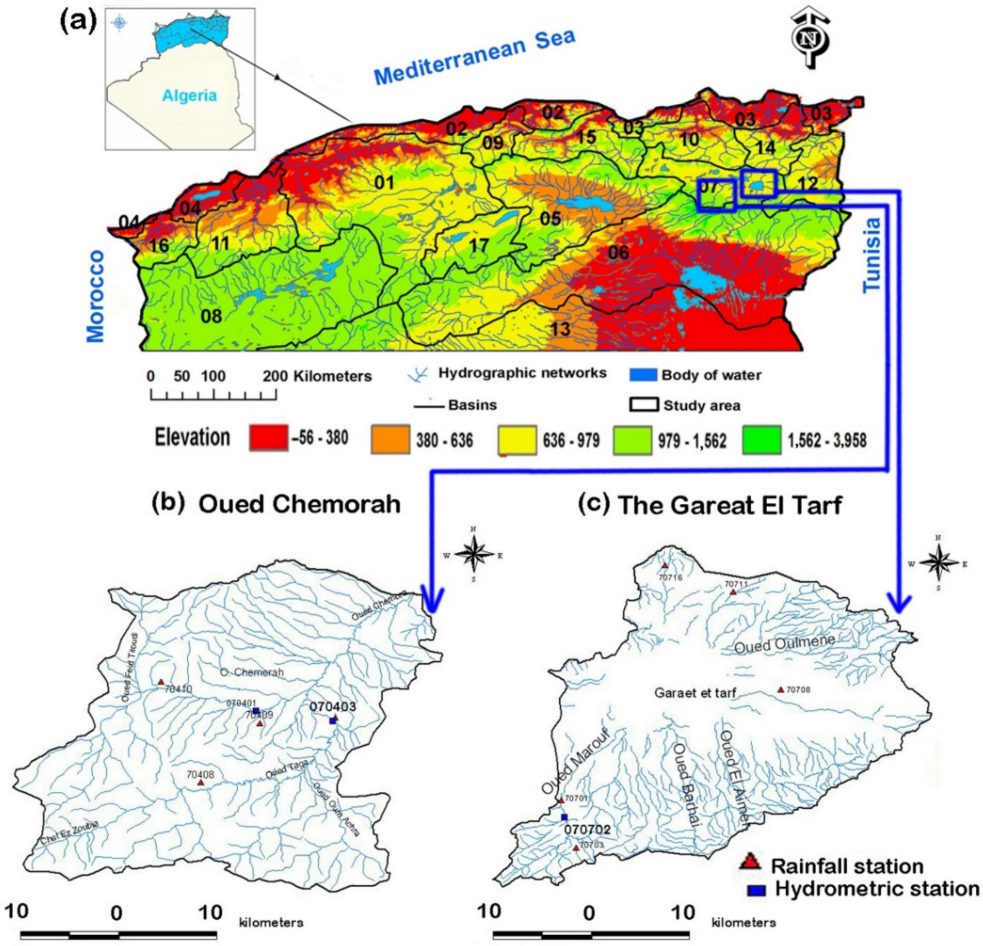

Figure 6. Geographic location of (**a**) Northern Algeria and (**b**,**c**) the main basins used in this study.

In this study, we used the hydrometric series of gauging stations of Foum El Gueiss coded 07-07-02 by ANRH. The data correspond to 1002 observations of flows and SSL of the Gueiss River during the flood events from 17 September 1971 to 11 January 1996, whereas the hydrometric series of the gauging station of Chemorah basin coded 07-04-03, also during the flood period, are from 17 August 1985 to 11 June 1997. Table 1 shows an example of the data used in this research. Note that the flow (Q_l) is obtained from the rating curve and the SSL (Q_s) is the product of Q_l by the corresponding suspended sediment concentration. The main statistical parameters for the data used in this study are presented in Table 2. According to Table 2, it can be said that the statistical characteristics of the data represented by the mean, standard deviation (STD), coefficient of variation (CV), minimum value (Min), and maximum value (Max) are relatively similar, with a slight difference in both Chemorah and Gareat el tarf basins.

Table 1. Example of the data used in this research.

Year	Month	Day	Hour	Height (m)	Q_l (m^3/s)	Q_s (kg/s)
1972	5	24	19:15	32	27.300	25.662
1972	5	25	06:30	17	0.966	0.985
1972	6	10	05:00	17	0.270	1.220
1972	6	11	06:00	17	0.270	0.837
1972	6	12	06:50	9	0.270	0.772
1972	7	17	05:40	8	0.098	0.632
1972	7	18	06:15	7	0.079	0.021
1972	7	19	19:00	32	0.062	0.786

Table 2. The statistical characteristics of river flow and SSL used in the study.

Basin	Statistical Parameters	Mean	STD	CV	Min	Max
Chemourah	Q_l (m^3/s)	4.7282	9.4349	1.9955	0	74.3000
	Q_s (kg/s)	71.1296	150.1295	2.1106	0	955.0040
Garaet el tarf	Q_l (m^3/s)	3.4225	7.3479	2.1470	0	69.5000
	Q_s (kg/s)	64.3165	162.9772	2.5340	0	957.6070

4. Evaluation Criteria

Models are generally evaluated in the training and validation phases by calculating the error between simulated and observed values using statistical parameters. The statistical parameters used in this research are root mean square error (RMSE), Theil's inequality coefficient (U^2) [54], the Nash–Sutcliffe efficiency coefficient (E) [55], and the correlation coefficient (R) [56]. The following equations define these criteria:

$$\mathrm{RMSE} = \sqrt{\frac{\sum_{i=1}^{N} \left(Qs_i - \hat{Q}s_i\right)^2}{N}} \tag{4}$$

$$\mathrm{U}^2 = \frac{\sum_{i=1}^{N} \left(Qs_i - \hat{Q}s_i\right)^2}{\sum_{i=1}^{N} Qs_i^2} \tag{5}$$

$$\mathrm{E} = 1 - \frac{\sum_{i=1}^{N} \left(Qs_i - \hat{Q}s_i\right)^2}{\sum_{i=1}^{N} \left(Qs_i - \overline{Q}s_i\right)^2} \tag{6}$$

$$\mathrm{R} = \frac{\sum_{i=1}^{N} \left(Qs_i - \overline{Q}s_i\right)\left(\hat{Q}s_i - \widetilde{Q}s_i\right)}{\sqrt{\sum_{i=1}^{N} \left(Qs_i - \overline{Q}s_i\right)^2 \sum_{i=1}^{N} \left(\hat{Q}s_i - \widetilde{Q}s_i\right)^2}} \tag{7}$$

where Qs_i is the measured value of SSL; $\hat{Q}s_i$ is the calculated SSL by the model; $\overline{Q}s_i$ is the measured average SSL; $\widetilde{Q}s_i$ is the calculated average SSL, and N is the number of data points.

5. Models Development

In this study, the neuro-particle swarm (ANN-PSO), neuro-fuzzy-particle swarm (ANFIS-PSO), RF, and LSTM models were used to estimate the SSL in the Gueiss and Chemourah rivers. Due to the lack of sufficient information in this study, flows with lag time t, t −−1, and t − 2 (Q_l(t), $-Q_l$(t − 1) and $-Q_l$(t − 2)) and SSL with lag time t − 1 (Q_s(t − 1)) were used as input vectors for the models, which are values observed during periods of flood events. The outputs of the models are the current calculated SSL (Q_s(t)) using water discharge and suspended sediment concentration.

The available database was divided into two sets to adjust model parameters and achieve optimal performance: a set for the training phase contains 70% of the data, and a set for the validation phase includes 30% of the data. Table 3 illustrates the combinations of the proposed input vectors to simulate the SSL by the ANN-PSO, ANFIS-PSO, RF, and LSTM models. For the ANN-PSO and ANFIS-PSO models, MLP and ANFIS were used in conjunction with the PSO optimization algorithm, as shown in Figure 3.

Table 3. The combinations of the proposed input vectors for ANN-PSO, ANFIS-PSO, RF, and LSTM.

Input Models	Number of Input	Output
(1) Q_l(t)	1	Q_s(t)
(2) Q_l(t) and –Q_s(t − 1)	2	Q_s(t)
(3) Q_l(t) and $-Q_l$(t − 1)	2	Q_s(t)
(4) Q_l(t), $-Q_l$(t − 1) and $-Q_s$(t − 1)	3	Q_s(t)
(5) Q_l(t), $-Q_l$(t − 1) and $-Q_l$(t − 2)	3	Q_s(t)
(6) Q_l(t), $-Q_l$(t − 1), $-Q_l$(t − 2) and $-Q_s$(t − 1)	4	Q_s(t)

ANN-PSO development is carried out by determining the optimum number of neurons in the hidden layer for different combinations of the proposed input vectors. This procedure was carried out by error testing by modifying the number of hidden neurons to obtain the structure that gives maximum performance. ANFIS-PSO was developed by performing error tests with variations in the number of rules for the input vector combinations provided. The rules that produced the slightest performance error were chosen to develop ANFIS-PSO to estimate SSL. We used the early stopping algorithm to avoid the over-fitting and under-fitting problem for the models used in this research (ANN-PSO and ANFIS-PSO). The early stopping algorithm determines the number of iterations and stops learning before the algorithm converges. It involves specifying the number of iterations used in training, checking for errors based on validation, and stopping training as soon as the error begins to increase. We follow the same process by error-testing the validation dataset of different sets of combinations input vectors proposed to develop RF and LSTM models to obtain the best possible performance for estimating SSL.

6. Results and Discussion

After developing ANN-PSO, ANFIS-PSO, RF, and LSTM models for different combinations of input vectors, they were evaluated according to RMSE error. In Chemourah basin, the ANN-PSO and LSTM models gave the lowest values for RMSE with a combination of input vectors (4 vectors). In contrast, the ANFIS-PSO model gave the highest values of RMSE for input vectors (4 vectors) for the two basins (Figure 7a). According to Figure 7b, in the Gareat el tarf basin, ANN-PSO and LSTM models had the lowest RMSE values with a combination of 4 input vectors, while RF and ANN-PSO models showed the lowest values for the combination of 2 and 3 input vectors, respectively.

Table 4 presents the results obtained by the optimal models of ANN-PSO, ANFIS-PSO, RF, and LSTM in the training and validation phases. According to Table 4, the ANN-PSO model provided the best results in estimating the SSL for both basins in the validation phase, i.e., RMSE = 67.2990 kg/s in Chemourah basin and RMSE = 55.8737 kg/s in Gareat el tarf basin. In contrast, the ANFIS-PSO model provided the worst results in both basins, i.e., RMSE = 158.2035 kg/s in Chemourah basin and RMSE = 165.3653 kg/s

in Gareat el tarf basin. The RF and LSTM models always gave acceptable results in the validation phase. In Chemourah basin, the RF model gave RMSE = 74.5747 kg/s and the LSTM model gave RMSE = 69.4178 kg/s, while in the Gareat el tarf basin the RF model gave the result of RMSE = 58.9957 kg/s and the LSTM model gave RMSE = 64.8888 kg/s. According to Kaveh et al. (2021) [29], the LSTM algorithm could satisfactorily predict SSC compared to ANN and ANFIS. Al Dahoul et al. (2021) [57] reported that LSTM outperformed other models such as linear regression, MLP, and extreme gradient boosting for SSL prediction. Sharafati et al. (2020) [58] applied new ensemble machine learning models for daily SSL prediction based on gradient boost regression (GBR), AdaBoost regression (ABR), and RF regression. This shows that the RF model has a slight lead in prediction performance.

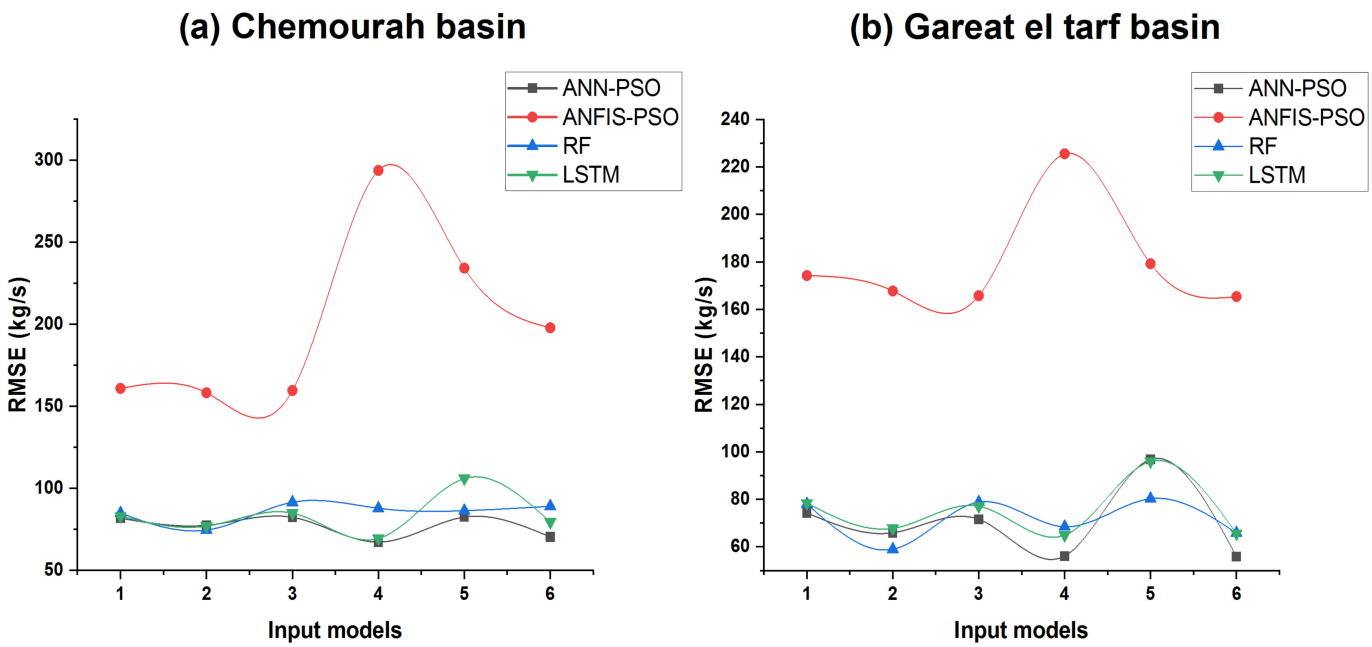

Figure 7. Evaluation of RMSE based on the different combinations of input vectors s for ANN-PSO, ANFIS-PSO, RF, and LSTM models in the validation phase.

Figures 8 and 9 show the superiority of the ANN-PSO, RF, and LSTM models over the ANFIS-PSO model. This superiority is translated by the results reported for the RMSE, U^2, E, and R statistical parameters (Table 4). In an in-depth comparison, the ANN-PSO model provides the best performance compared with the other models with low values of RMSE and U^2, and high values of E and R. Similarly, Mohammadi et al. (2021) [59] concluded that ANN-PSO is the best algorithm in terms of accurate prediction of SSL with a lower number of input parameters compared to radial basis function (RBFNN) and SVM. Hanoon et al. (2021) [60] revealed that ANN provided a superior performance to that of the gradient boost regression (GBT), RF, and SVM for SSL prediction for some case studies in Malaysia. Idrees et al. (2021) [61] concluded that the ANN is better compared to the ANFIS, RBFNN, SVM , and GP in terms of SSL prediction capabilities. Nhu et al. 2020 [62] tested the predictive ability of a random subspace (RS), RF, two SVM models using a radial basis function kernel (SVM-RBF) and a normalized polynomial kernel (SVM-NPK) model for monthly SSL estimation. The results show the superiority of the RS model compared to SVM-RBF, SVM-NPK, and RF models. Ehteram et al. 2021 [63] optimized ANN by multi-objective whale algorithm (MOWA) for predicting daily SSL. The ANN-MOWA model showed the best accuracy for predicting daily SSL, compared with other models. The main statistical characteristics of mean, standard deviation (STD), coefficient of variation (CV), minimum value (Min), and maximum value (Max) of the observed and estimated SSL by the optimum models

of ANN, ANFIS, ANN-GA, and ANN-PSO in the training and validation phases are shown in Table 5. Figures 10 and 11 show comparisons between observed and estimated SSL values using the optimal ANN-PSO, ANFIS-PSO, RF, and LSTM models (training and validation phases). These figures demonstrate the efficacy and superiority of the ANN-PSO, RF, and LSTM models compared to ANFIS-PSO. The poor results obtained by ANFIS-PSO are due to the complexity of the fuzzy rules, which led the model to not find a well-defined relationship between inputs and outputs.

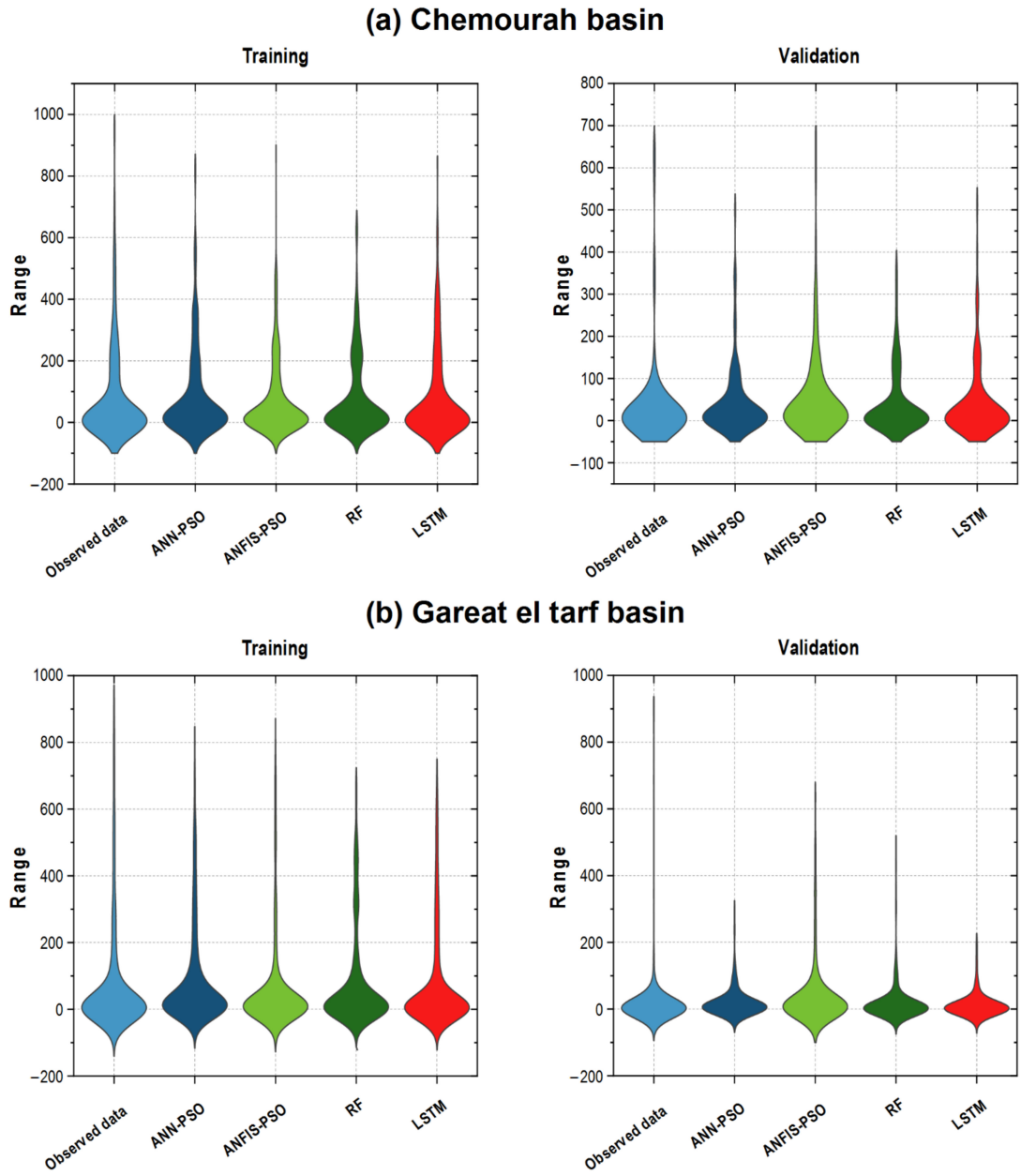

Figure 8. Violin diagram of different machine learning models in the training and validation phases.

From Table 4 and Figures 10 and 11, the ANN-PSO model has provided more efficient results than the RF, LSTM, and ANFIS-PSO models for estimating SSL. Comparing the obtained results with those presented by Bouzeria et al. (2017) [64], using data from northeastern Algeria to predict sediment loads in the Mellah catchment with an ANN, the present results are very satisfactory, despite the lack of sufficient information and the use of only recorded flood data.

Table 4. The results obtained by ANN-PSO, ANFIS-PSO, RF, and LSTM for the training and validation phases.

Basin	Models	Phases	RMSE	U^2	E	R
Chemourah	ANN-PSO	Training	78.1193	0.1828	0.7663	0.8755
		Validation	67.2990	0.3274	0.6346	0.8003
	ANFIS-PSO	Training	201.5912	1.2171	−0.5561	0.0051
		Validation	158.2035	1.8090	−1.0195	−0.0012
	RF	Training	77.1006	0.1780	0.7724	0.8845
		Validation	74.5747	0.4020	0.5513	0.7458
	LSTM	Training	62.0405	0.1153	0.8526	0.9239
		Validation	69.4178	0.3483	0.6112	0.7824
Garaet el tarf	ANN-PSO	Training	88.7852	0.2009	0.7564	0.8706
		Validation	55.8737	0.2904	0.6971	0.8392
	ANFIS-PSO	Training	239.5296	1.4647	−0.7753	−0.0235
		Validation	165.3653	2.5346	−1.6440	−0.0394
	RF	Training	80.1885	0.1639	0.8013	0.8974
		Validation	58.9957	0.3237	0.6624	0.8157
	LSTM	Training	68.6353	0.1201	0.8544	0.9273
		Validation	64.8888	0.3916	0.5915	0.7706

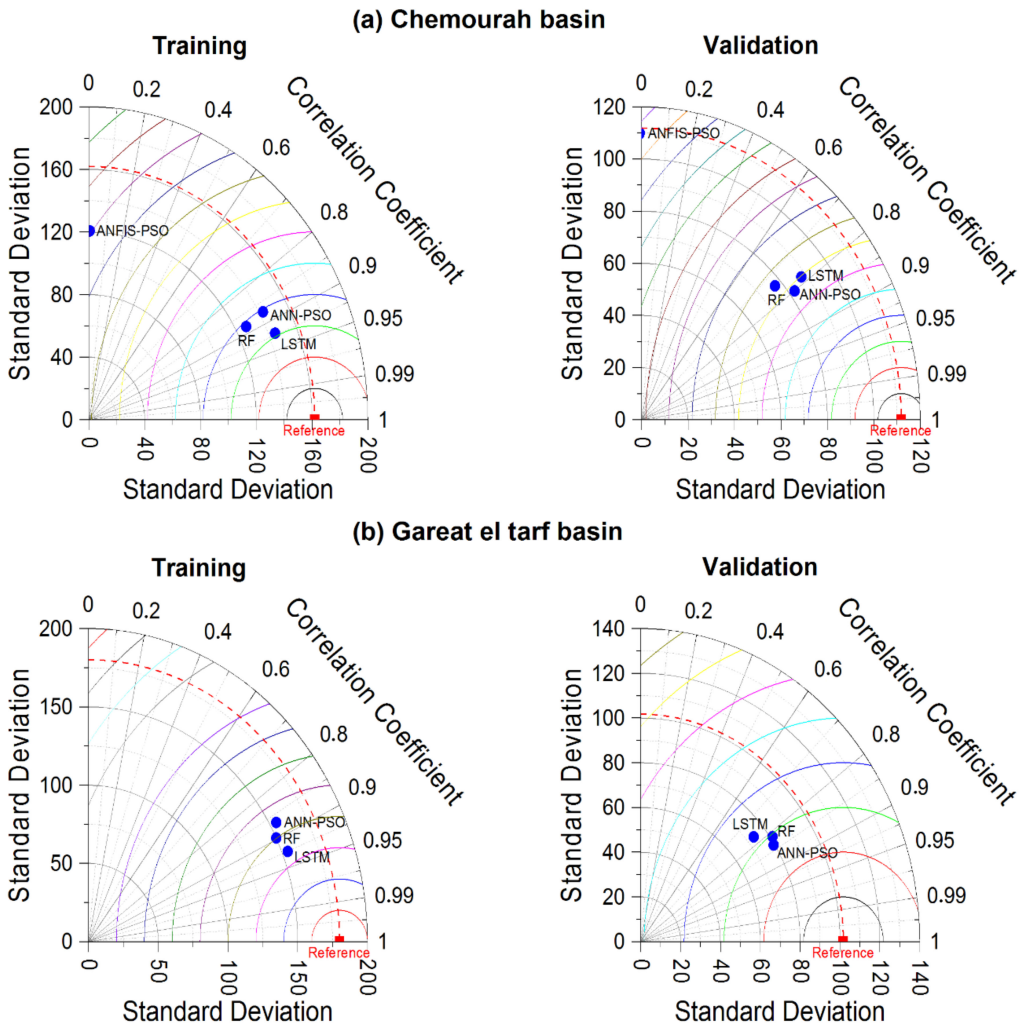

Figure 9. Taylor diagram of different machine learning models in the training and validation phases.

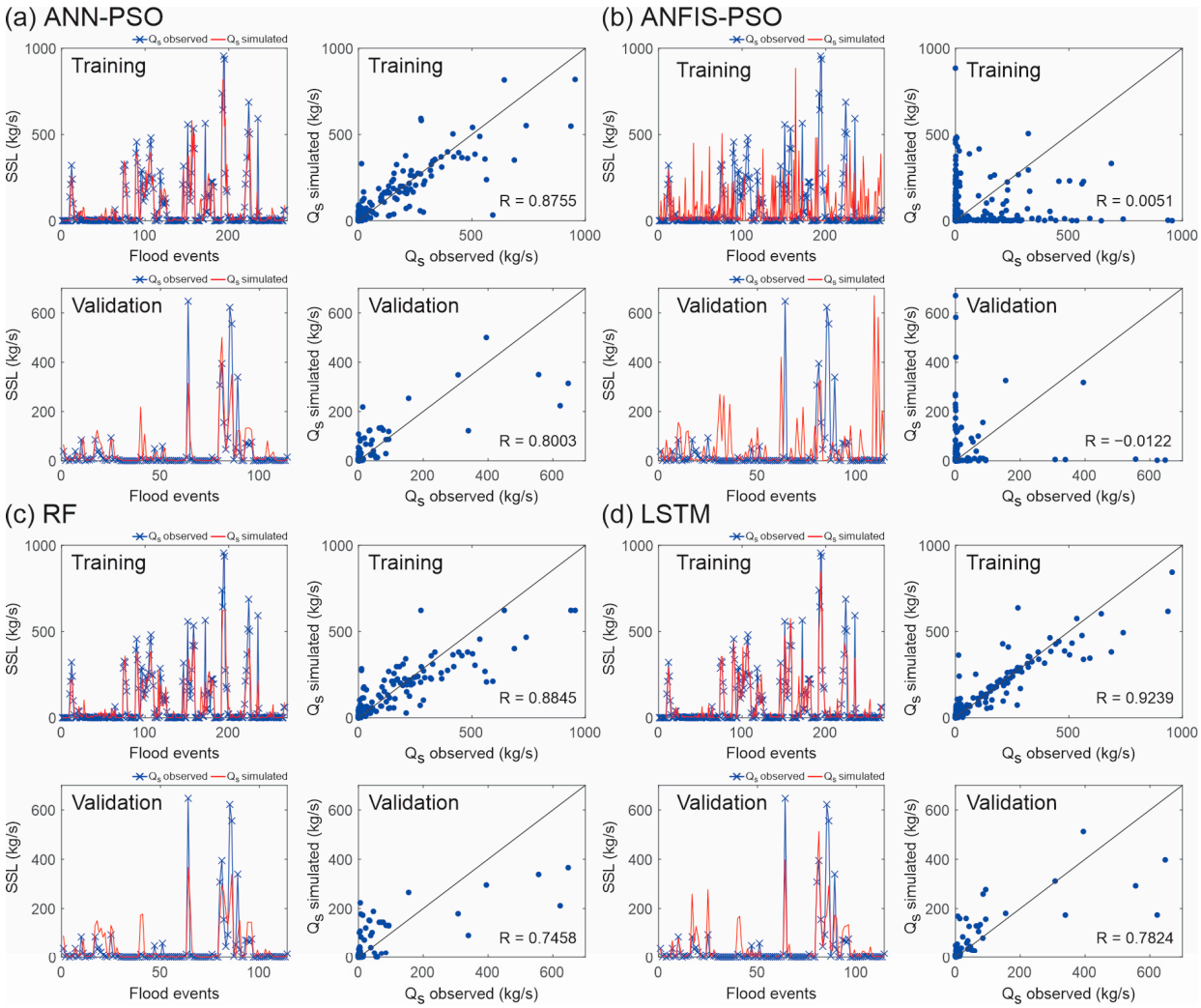

Figure 10. Comparison between observed and estimated SSL of Chemourah basin by the different machine learning models in the training and validation phases.

Table 5. Characteristics of statistical parameters of observed and estimated SSL for ANN-PSO, ANFIS-PSO, RF, and LSTM.

Basin	Models	Phases	Flow	Mean	STD	CV	Min	Max
Chemourah	ANN−PSO	Training	Observed	85.2852	161.9096	1.8984	0	955.0040
			Simulated	87.2012	142.5901	1.6352	0.0567	819.1319
		Validation	Observed	37.9759	111.8170	2.9444	0	647.2060
			Simulated	42.6991	82.3302	1.9282	0.1968	500.3120
	ANFIS−PSO	Training	Observed	85.2852	161.9096	1.8984	0	955.0040
			Simulated	71.0791	120.7254	1.6985	−0.0036	884.2506
		Validation	Observed	37.9759	111.8170	2.9444	0	647.2060
			Simulated	56.9000	109.9396	1.9322	0.0252	670.2476
	RF	Training	Observed	85.2852	161.9096	1.8984	0	955.0040
			Simulated	81.5454	127.4940	1.5635	0.0486	622.4522
		Validation	Observed	37.9759	111.8170	2.9444	0	647.2060
			Simulated	42.5403	77.0234	1.8106	0.0486	365.7755
	LSTM	Training	Observed	85.2852	161.9096	1.8984	0	955.0040
			Simulated	84.1479	144.4213	1.7163	−52.7124	843.7532
		Validation	Observed	37.9759	111.8170	2.9444	0	647.2060
			Simulated	41.4518	87.9488	2.1217	−17.5058	512.4590

Table 5. *Cont.*

Basin	Models	Phases	Flow	Mean	STD	CV	Min	Max
Garaet el tarf	ANN−PSO	Training	Observed	82.9021	180.0103	2.1714	0	957.6070
			Simulated	89.6066	154.6680	1.7261	0.0427	859.5337
		Validation	Observed	21.0568	101.7052	4.8301	0	909.5410
			Simulated	27.2904	79.4557	2.9115	0.0310	776.1455
	ANFIS−PSO	Training	Observed	82.9021	180.0103	2.1714	0	957.6070
			Simulated	64.5640	153.1941	2.3727	−111.9880	931.0246
		Validation	Observed	21.0568	101.7052	4.8301	0	909.5410
			Simulated	45.9378	124.2811	2.7054	−0.0695	1.1821
	RF	Training	Observed	82.9021	180.0103	2.1714	0	957.6070
			Simulated	82.6496	150.0450	1.8154	0.0721	687.6447
		Validation	Observed	21.0568	101.7052	4.8301	0	909.5410
			Simulated	26.3224	81.1212	3.0818	0.0721	641.6942
	LSTM	Training	Observed	82.9021	180.0103	2.1714	0	957.6070
			Simulated	79.1898	154.0421	1.9452	−32.8914	739.1696
		Validation	Observed	21.0568	101.7052	4.8301	0	909.5410
			Simulated	21.2770	73.5315	3.4559	−39.5889	711.1299

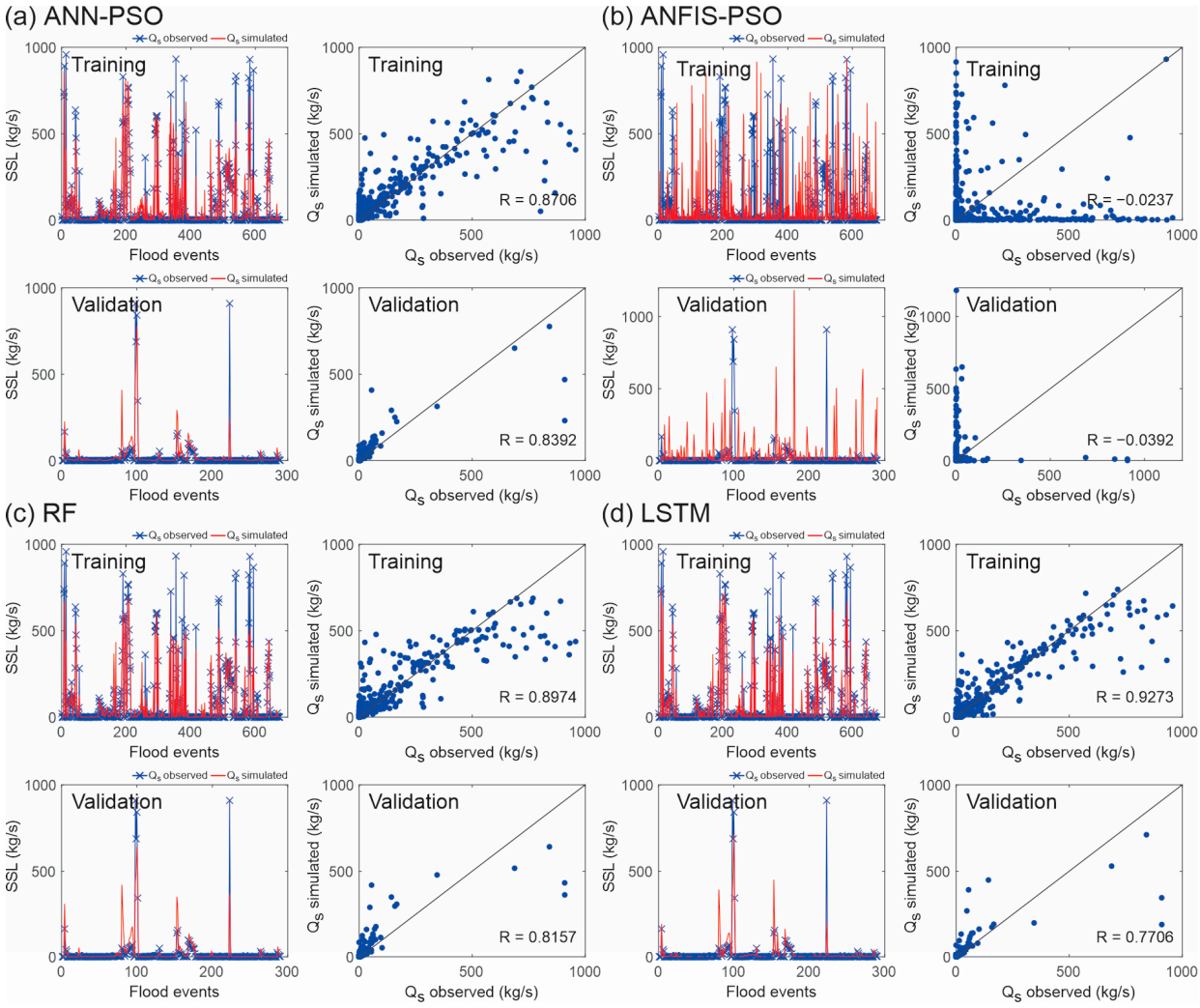

Figure 11. Comparison between observed and estimated SSL of Gareat el tarf basin by the different machine learning models in the training and validation phases.

7. Conclusions

In this study, four different machine learning approaches, ANN-PSO, ANFIS-PSO, RF, and LSTM, were examined for estimating SSL in the Chemourah and Gareat el tarf basins using observation data of flood events of the Chemourah and Gueiss rivers. This paper also shows that the ANN-PSO, RF, and LSTM models have given a better accuracy of simulations compared to the ANFIS-PSO model. Model performances were measured using RMSE, U^2, E, and R, between the estimated and observed SSL values. The results indicate that the ANN-PSO model is slightly better than the RF and LSTM models for estimating SSL in the Chemourah and Gareat el tarf basins. We concluded from this study that the ANN-PSO, RF, and LSTM models can always give good results compared with the ANFIS-PSO model. The ANN-PSO, RF, and LSTM models can decrease the complexity of runoff and SSL relationships and increase the estimation accuracy. These encouraging results lead us to experiment and use other machine learning systems and hybrid models to estimate SSL in rivers, and encourage the installation of flumes that enable more accurate measurements in the basin outlet sections to take even more advantage of such new computational techniques.

Author Contributions: Z.A., B.Z., M.A. and M.C. conceived the framework of this research, processed data, designed the experiments, plots, and map preparation, validated the processing results, and wrote the manuscript. C.A.G.S. and E.E.H. gave feedback on the written manuscript and helped to analyze and edit the manuscript for proper English language, grammar, punctuation, spelling, and technical improvements. All authors have read and agreed to the published version of the manuscript.

Funding: This research was funded by Taif University, Researchers Supporting Project, grant number TURSP-2020/324.

Institutional Review Board Statement: Not applicable.

Informed Consent Statement: Not applicable.

Data Availability Statement: The data that support the findings of this study are available from the corresponding author Bilel Zerouali, upon reasonable request.

Acknowledgments: Authors would like to acknowledge the financial support provided from Taif University Researchers Supporting Project, grant number TURSP-2020/324. The authors gratefully thank the Directorate General for Scientific Research and Technological Development and the National Agency of Water Resources (ANRH) of Algeria who gave us the needed data to realize this research.

Conflicts of Interest: The authors declare no conflict of interest.

References

1. ONU. 2020. Available online: www.greenfacts.org/fr/ressources-eau/ (accessed on 2 March 2020).
2. Khan, M.Y.A.; Tian, F.; Hasan, F.; Chakrapani, G.J. Artificial neural network simulation for prediction of suspended sediment concentration in the River Ramganga, Ganges Basin, India. *Int. J. Sediment Res.* **2019**, *34*, 95–107. [CrossRef]
3. Zounemat-Kermani, M.; Kişi, Ö.; Adamowski, J.; Ramezani-Charmahineh, A. Evaluation of data driven models for river suspended sediment concentration modeling. *J. Hydrol.* **2016**, *535*, 457–472. [CrossRef]
4. Salih, S.-Q.; Sharafati, A.; Khosravi, K.; Faris, H.; Kisi, O.; Tao, H.; Yaseen, Z.-M. River suspended sediment load prediction based on river discharge information: Application of newly developed data mining models. *Hydrol. Sci. J.* **2020**, *65*, 624–637. [CrossRef]
5. Kisi, Ö. Multi-layer perceptrons with Levenberg-Marquardt training algorithm for suspended sediment concentration prediction and estimation/Prévision et estimation de la concentration en matières en suspension avec des perceptrons multi-couches et l'algorithme d'apprentissage de Levenberg-Marquardt. *Hydrol. Sci. J.* **2004**, *49*, 1025–1040. [CrossRef]
6. Toumi, A.; Remini, B. Perte de la capacité de stockage d'eau au barrage de Beni Haroun, Algérie. Loss of water storage capacity at the Beni Haroun dam, Algeria. *Syst. Agric. Environ.* **2018**, *2*, 80–97.
7. Remini, B.; Bensafia, D.; Mekhatri, A. Sidi M'hamed Ben Aouda's Dam (Algeria): Acceleration to the silting! *LARHYSS* **2018**, *33*, 221–252.
8. Yilmaz, B.; Aras, E.; Kankal, M.; Nacar, S. Prediction of suspended sediment loading by means of hybrid artificial intelligence approaches. *Acta Geophys.* **2019**, *67*, 1693–1705. [CrossRef]

9. Zerouali, B.; Chettih, M.; Abda, Z.; Mesbah, M.; Djemai, M. The use of hybrid methods for change points and trends detection in rainfall series of northern Algeria. *Acta Geophys.* **2020**, *68*, 1443–1460. [CrossRef]
10. Abda, Z.; Chettih, M. Forecasting daily flow rate-based intelligent hybrid models combining wavelet and Hilbert–Huang transforms in the mediterranean basin in northern Algeria. *Acta Geophys.* **2018**, *66*, 1131–1150. [CrossRef]
11. Abda, Z.; Chettih, M.; Zerouali, B. Assessment of neuro-fuzzy approach based different wavelet families for daily flow rates forecasting. *Model. Earth Syst. Environ.* **2020**, *7*, 1523–1538. [CrossRef]
12. Bajirao, T.S.; Kumar, P.; Kumar, M.; Elbeltagi, A.; Kuriqi, A. Superiority of Hybrid Soft Computing Models in Daily Suspended Sediment Estimation in Highly Dynamic Rivers. *Sustainability* **2021**, *13*, 542. [CrossRef]
13. Cimen, M. Estimation of daily suspended sediments using support vector machines. *Hydrol. Sci. J.* **2008**, *53*, 656–666. [CrossRef]
14. Ghorbani, M.A.; Khatibi, R.; Singh, V.P.; Kahya, E.; Ruskeepää, H.; Saggi, M.K.; Sivakumar, B.; Kim, S.; Salmasi, F.; Kashani, M.H.; et al. Continuous monitoring of suspended sediment concentrations using image analytics and deriving inherent correlations by machine learning. *Sci. Rep.* **2020**, *10*, 1–9.
15. Azamathulla, H.M.; Cuan, Y.C.; Ghani, A.A.; Chang, C.K. Suspended sediment load prediction of river systems: GEP approach. *Arab. J. Geosci.* **2013**, *6*, 3469–3480. [CrossRef]
16. Lafdani, E.K.; Nia, A.M.; Ahmadi, A. Daily suspended sediment load prediction using artificial neural networks and support vector machines. *J. Hydrol.* **2013**, *478*, 50–62. [CrossRef]
17. Olyaie, E.; Banejad, H.; Chau, K.W.; Melesse, A.M. A comparison of various artificial intelligence approaches performance for estimating suspended sediment load of river systems: A case study in United States. *Environ. Monit. Assess.* **2015**, *187*, 1–22. [CrossRef] [PubMed]
18. Shamaei, E.; Kaedi, M. Suspended sediment concentration estimation by stacking the genetic programming and neuro-fuzzy predictions. *Appl. Soft. Comput.* **2016**, *45*, 187–196. [CrossRef]
19. Buyukyildiz, M.; Kumcu, S.Y. An estimation of the suspended sediment load using adaptive network based fuzzy inference system, support vector machine and artificial neural network models. *Water Resour. Manag.* **2017**, *31*, 1343–1359. [CrossRef]
20. Elahcene, O.; Bouznad, I.E.; Bouleknaft, Z. Erosion and solid transport processes in the Isser Wadi watershed, Algeria. *Euro-Mediterr. J. Environ. Integr.* **2019**, *4*, 1–10. [CrossRef]
21. Kisi, O.; Yaseen, Z.M. The potential of hybrid evolutionary fuzzy intelligence model for suspended sediment concentration prediction. *Catena* **2019**, *174*, 11–23. [CrossRef]
22. Nourani, V.; Molajou, A.; Tajbakhsh, A.D.; Najafi, H. A wavelet based data mining technique for suspended sediment load modeling. *Water Resour. Manag.* **2019**, *33*, 1769–1784. [CrossRef]
23. Nourani, V.; Andalib, G. Daily and monthly suspended sediment load predictions using wavelet based artificial intelligence approaches. *J. Mt. Sci.* **2015**, *12*, 85–100. [CrossRef]
24. Asheghi, R.; Hosseini, S.A.; Saneie, M.; Shahri, A.-A. Updating the neural network sediment load models using different sensitivity analysis methods: A regional application. *J. Hydroinf.* **2020**, *22*, 562–577. [CrossRef]
25. Meshram, S.G.; Ghorbani, M.A.; Deo, R.C.; Kashani, M.H.; Meshram, C.; Karimi, V. New approach for sediment yield forecasting with a two-phase feedforward neuron network-particle swarm optimization model integrated with the gravitational search algorithm. *Water Resour. Manag.* **2019**, *33*, 2335–2356. [CrossRef]
26. Kumar, D.; Pandey, A.; Sharma, N.; Flügel, W.A. Daily suspended sediment simulation using machine learning approach. *Catena* **2016**, *138*, 77–90. [CrossRef]
27. Adnan, R.-M.; Liang, Z.; El-Shafie, A.; Zounemat-Kermani, M.; Kisi, O. Prediction of suspended sediment load using data-driven models. *Water* **2019**, *11*, 2060. [CrossRef]
28. Banadkooki, F.B.; Ehteram, M.; Ahmed, A.N.; Teo, F.Y.; Ebrahimi, M.; Fai, C.M.; Huang, Y.K.; El-Shaife, A. Suspended sediment load prediction using artificial neural network and ant lion optimization algorithm. *Environ. Sci. Pollut. Res.* **2020**, *27*, 38094–38116. [CrossRef] [PubMed]
29. Kaveh, K.; Kaveh, H.; Bui, M.-D.; Rutschmann, P. Long short-term memory for predicting daily suspended sediment concentration. *Eng. Comput.* **2020**, *37*, 2013–2027. [CrossRef]
30. Zerouali, B.; Chettih, M.; Abda, Z.; Mesbah, M.; Santos, C.A.G.; Neto, R.M.B.; da Silva, R.M. Spatiotemporal meteorological drought assessment in a humid Mediterranean region: Case study of the Oued Sebaou basin (northern central Algeria). *Nat. Hazards* **2021**, *108*, 689–709. [CrossRef]
31. Touati, B. Les Barrages et la Politique Hydraulique en Algérie. 2010. Available online: https://bu.umc.edu.dz/theses/sc-terre/TOU5850.pdf (accessed on 5 July 2021).
32. Zerouali, B.; Chettih, M.; Alwetaishi, M.; Abda, Z.; Elbeltagi, A.; Augusto Guimarães Santos, C.; Hussein, E.E. Evaluation of Karst Spring Discharge Response Using Time-Scale-Based Methods for a Mediterranean Basin of Northern Algeria. *Water* **2021**, *13*, 2946. [CrossRef]
33. Baosheng, W.U.; Van Maren, D.S.; Lingyun, L.-I. Predictability of sediment transport in the Yellow River using selected transport formulas. *Inter. J. Sediment Res.* **2008**, *23*, 283–298.
34. Benkhaled, A.; Remini, B. Variabilité temporelle de la concentration en sédiments et phénomène d'hystérésis dans le bassin de l'Oued Wahrane (Algérie). *Hydrol. Sci. J.* **2003**, *48*, 243–255. [CrossRef]
35. El Mahi, A.; Meddi, M.; Bravard, J.P. Analyse du transport solide en suspension dans le bassin versant de l'Oued El Hammam (Algérie du Nord). *Hydrol. Sci. J.* **2012**, *57*, 1642–1661. [CrossRef]

36. Nakato, T. Tests of selected sediment-transport formulas. *J. Hydraul. Eng.* **1990**, *116*, 362–379. [CrossRef]
37. Hasbaia, M.; Paquier, A.; Herizi, T. Hydrological modeling of sediment transport in the semiarid region, case of Soubella watershed in Algeria. In *Water Resources in Arid Areas: The Way Forward*; Springer: Cham, Switzerland, 2017; pp. 251–266.
38. Tachi, S.E.; Bouguerra, H.; Derdous, O.; Djabri, L.; Benmamar, S. Estimating suspended sediment concentration at different time scales in Northeastern Algeria. *Appl. Water Sci.* **2020**, *10*, 1–8. [CrossRef]
39. Bouguerra, H.; Tachi, S.-E.; Derdous, O.; Bouanani, A.; Khanchoul, K. Suspended sediment discharge modeling during flood events using two different artificial neural network algorithms. *Acta Geophys.* **2019**, *67*, 1649–1660. [CrossRef]
40. Boukhrissa, Z.A.; Khanchoul, K.; Le Bissonnais, Y.; Tourki, M. Prediction of sediment load by sediment rating curve and neural network (ANN) in El Kebir catchment, Algeria. *J. Earth Syst. Sci.* **2013**, *122*, 1303–1312. [CrossRef]
41. Salhi, C.; Touaibia, B.; Zeroual, A. Les réseaux de neurones et la régression multiple en prédiction de l'érosion spécifique: Cas du bassin hydrographique Algérois-Hodna-Soummam (Algérie). *Hydrol. Sci. J.* **2013**, *58*, 1573–1580. [CrossRef]
42. Tachi, S.E.; Ouerdachi, L.; Remaoun, M.; Derdous, O.; Boutaghane, H. Forecasting suspended sediment load using regularized neural network: Case study of the Isser River (Algeria). *J. Water Land Develop.* **2016**, *29*, 75–81. [CrossRef]
43. Wu, C.L.; Chau, K.W.; Fan, C. Prediction of rainfall time series using modular artificial neural networks coupled with data-preprocessing techniques. *J. Hydrol.* **2010**, *389*, 146–167. [CrossRef]
44. Kim, R.J.; Loucks, D.P.; Stedinger, J.R. Artificial neural network models of watershed nutrient loading. *Water Resour. Manag.* **2012**, *26*, 2781–2797. [CrossRef]
45. Rezaeianzadeh, M.; Tabari, H.; Yazdi, A.-A.; Isik, S.; Kalin, L. Flood flow forecasting using ANN, ANFIS and regression models. *Neural Comput. Appl.* **2014**, *25*, 25–37. [CrossRef]
46. Jang, J.S. ANFIS: Adaptive-network-based fuzzy inference system. *IEEE Trans. Syst. Man Cybern.* **1993**, *23*, 665–685. [CrossRef]
47. Sugeno, M.; Kang, G.T. Fuzzy modelling and control of multilayer incinerator. *Fuzzy Set Syst.* **1986**, *18*, 329–345. [CrossRef]
48. Takagi, T.; Sugeno, M. Fuzzy identification of systems and its applications to modeling and control. *IEEE Trans. Syst. Man Cybern. SMC* **1985**, *1*, 116–132. [CrossRef]
49. Akrami, S.A.; El-Shafie, A.; Jaafar, O. Improving rainfall forecasting efficiency using modified adaptive neuro-fuzzy inference system (MANFIS). *Water Resour. Manag.* **2013**, *27*, 3507–3523. [CrossRef]
50. Awan, J.A.; Bae, D.H. Improving ANFIS based model for long-term dam inflow prediction by incorporating monthly rainfall forecasts. *Water Resour. Manag.* **2014**, *28*, 1185–1199. [CrossRef]
51. Kennedy, J.; Eberhart, R. Particle swarm optimization. In Proceedings of the ICNN'95—International Conference on Neural Networks, Perth, Australia, 27 November–1 December 1995; pp. 1942–1948.
52. Breiman, L. Random forests. *Mach. Learn.* **2001**, *45*, 5–32. [CrossRef]
53. Naouel, D.; Zouini, D.; Breil, P. Contribution to flood risk management by the IRIP method at the level of Gareat El Taref catchment, Constantine's highlands, North-East of Algeria. *J. Water Land Develop.* **2018**, *38*, 95–104. [CrossRef]
54. Hauduc, H.; Neumann, M.B.; Muschalla, D.; Gamerith, V.; Gillot, S.; Vanrolleghem, P.A. Efficiency criteria for environmental model quality assessment: A review and its application to wastewater treatment. *Environ. Modell. Soft.* **2015**, *68*, 196–204. [CrossRef]
55. Abda, Z.; Chettih, M.; Zerouali, B. Efficiency of a neuro-fuzzy model based on the Hilbert-Huang transform for flood prediction. In *Advances in Sustainable and Environmental Hydrology, Hydrogeology, Hydrochemistry and Water Resources*; Springer: Cham, Switzerland, 2019; pp. 401–404.
56. Kisi, O.; Latifoğlu, L.; Latifoğlu, F. Investigation of empirical mode decomposition in forecasting of hydrological time series. *Water Resour. Manag.* **2014**, *28*, 4045–4057. [CrossRef]
57. AlDahoul, N.; Essam, Y.; Kumar, P.; Ahmed, A.N.; Sherif, M.; Sefelnasr, A.; Elshafie, A. Suspended sediment load prediction using long short-term memory neural network. *Sci. Rep.* **2021**, *11*, 1–22.
58. Sharafati, A.; Haji Seyed Asadollah, S.B.; Motta, D.; Yaseen, Z.M. Application of newly developed ensemble machine learning models for daily suspended sediment load prediction and related uncertainty analysis. *Hydrol. Sci. J.* **2020**, *65*, 2022–2042. [CrossRef]
59. Mohammadi, B.; Guan, Y.; Moazenzadeh, R.; Safari, M.-J.S. Implementation of hybrid particle swarm optimization-differential evolution algorithms coupled with multi-layer perceptron for suspended sediment load estimation. *Catena* **2021**, *198*, 105024. [CrossRef]
60. Hanoon, M.S.; Abdullatif, A.A.B.; Ahmed, A.N.; Razzaq, A.; Birima, A.H.; El-Shafie, A.A. Comparison of various machine learning approaches performance for prediction suspended sediment load of river systems: A case study in Malaysia. *Earth Sci. Inform.* **2021**, 1–14. [CrossRef]
61. Idrees, M.B.; Jehanzaib, M.; Kim, D.; Kim, T.W. Comprehensive evaluation of machine learning models for suspended sediment load inflow prediction in a reservoir. *Stoch. Environ. Res. Risk. Assess.* **2021**, *35*, 1805–1823. [CrossRef]
62. Nhu, V.H.; Khosravi, K.; Cooper, J.R.; Karimi, M.; Kisi, O.; Pham, B.T.; Lyu, Z. Monthly suspended sediment load prediction using artificial intelligence: Testing of a new random subspace method. *Hydrol. Sci. J.* **2020**, *65*, 2116–2127. [CrossRef]
63. Ehteram, M.; Ahmed, A.N.; Latif, S.D.; Huang, Y.F.; Alizamir, M.; Kisi, O.; Mert, C.; El-Shafie, A. Design of a hybrid ANN multi-objective whale algorithm for suspended sediment load prediction. *Environ. Sci. Poll. Res.* **2021**, *28*, 1596–1611. [CrossRef] [PubMed]

64. Bouzeria, H.; Ghenim, A.N.; Khanchoul, K. Using artificial neural network (ANN) for prediction of sediment loads, application to the Mellah catchment, northeast Algeria. *J. Water Land Develop.* **2017**, *33*, 47–55. [CrossRef]